The Journal of Immunology

Human Cytomegalovirus Alters Localization of MHC Class II and Dendrite Morphology in Mature Langerhans Cells

Andrew W. Lee, Laura Hertel, Ryan K. Louie, Timo Burster, Vashti Lacaille, Achal Pashine, Davide A. Abate, Edward S. Mocarski and Elizabeth D. Mellins

J Immunol 2006; 177:3960-3971; ;
doi: 10.4049/jimmunol.177.6.3960
http://www.jimmunol.org/content/177/6/3960

The Journal of Immunology is published twice each month by
The American Association of Immunologists, Inc.,
1451 Rockville Pike, Suite 650, Rockville, MD 20852

Print ISSN: 0022-1767 Online ISSN: 1550-6606.

Human Cytomegalovirus Alters Localization of MHC Class II and Dendrite Morphology in Mature Langerhans Cells[1]

Andrew W. Lee,*§ Laura Hertel,[2]† Ryan K. Louie,‡ Timo Burster,* Vashti Lacaille,[3]* Achal Pashine,[4]* Davide A. Abate,† Edward S. Mocarski,† and Elizabeth D. Mellins[5]*

Hemopoietic stem cell-derived mature Langerhans-type dendritic cells (LC) are susceptible to productive infection by human CMV (HCMV). To investigate the impact of infection on this cell type, we examined HLA-DR biosynthesis and trafficking in mature LC cultures exposed to HCMV. We found decreased surface HLA-DR levels in viral Ag-positive as well as in Ag-negative mature LC. Inhibition of HLA-DR was independent of expression of unique short US2-US11 region gene products by HCMV. Indeed, exposure to UV-inactivated virus, but not to conditioned medium from infected cells, was sufficient to reduce HLA-DR on mature LC, implicating particle binding/penetration in this effect. Reduced surface levels reflected an altered distribution of HLA-DR because total cellular HLA-DR was not diminished. Accumulation of HLA-DR was not explained by altered cathepsin S activity. Mature, peptide-loaded HLA-DR molecules were retained within cells, as assessed by the proportion of SDS-stable HLA-DR dimers. A block in egress was implicated, as endocytosis of surface HLA-DR was not increased. Immunofluorescence microscopy corroborated the intracellular retention of HLA-DR and revealed markedly fewer HLA-DR-positive dendritic projections in infected mature LC. Unexpectedly, light microscopic analyses showed a dramatic loss of the dendrites themselves and immunofluorescence revealed that cytoskeletal elements crucial for the formation and maintenance of dendrites are disrupted in viral Ag-positive cells. Consistent with these dendrite effects, HCMV-infected mature LC exhibit markedly reduced chemotaxis in response to lymphoid chemokines. Thus, HCMV impedes MHC class II molecule trafficking, dendritic projections, and migration of mature LC. These changes likely contribute to the reduced activation of CD4$^+$ T cells by HCMV-infected mature LC. ***The Journal of Immunology,*** **2006, 177: 3960–3971.**

Human CMV (HCMV)[6] is a highly prevalent betaherpesvirus that causes latent infection in immunocompetent individuals. In the developing fetus, immunocompromised transplant recipients, and patients with AIDS, HCMV may disseminate widely and cause significant morbidity and mortality (reviewed in Ref. 1).

A critical component of the host immune response to HCMV infection and reactivation is mediated by CD4$^+$ T cells. These cells are direct antiviral effectors and also provide help for maintenance of CD8$^+$ T cell responses (2). Asymptomatic HCMV-infected young children, who are a major reservoir for HCMV transmission due to their prolonged viral shedding, display a selective defect in HCMV-specific CD4$^+$ T cells (3). This finding is reminiscent of results with murine CMV, in which eradication of virus from tissue sites, such as salivary glands, is dependent on CD4$^+$ T cell-secreted IFN-γ (4). The induction of murine CMV-specific CD8$^+$ T cell cytotoxic immunity also requires CD4$^+$ T cells (5).

The priming of MHC class II-restricted CD4$^+$ T cells by professional APCs is thus crucial for control of HCMV infection. Notably, HCMV directly infects professional APC, including monocytes (6), macrophages (7), and dendritic cells (DCs) (8–10). In addition, myeloid lineage precursors of these cells provide an important site for HCMV latency (11, 12), and reactivation of viral replication is thought to be associated with differentiation of precursors into APCs (13). These scenarios have led to the hypothesis that HCMV may modulate the MHC class II pathway for immune evasion.

Studies of HCMV interaction with MHC class II molecules have been conducted in both primary cells (14) and model systems in which MHC class II genes are introduced by gene transfer (15, 16). These studies differ in their identified mechanisms for MHC class II modulation by HCMV, which may be attributed to differences in experimental system and/or cell type studied. Our studies have focused on primary Langerhans-type DCs, referred to as Langerhans cells (LC). These cells are of particular interest because of their location in skin and mucosal surfaces, where primary contact with mucosally acquired pathogens like HCMV typically occurs. We have used a well-described in vitro cell culture system in which immature LC are derived by cytokine stimulation of CD34$^+$ hemopoietic progenitors and then stimulated to mature by exposure to CD40L (17–19). Previously, we showed that infection by

*Department of Pediatrics, †Department of Microbiology and Immunology, ‡Department of Molecular and Cellular Physiology, and §Department of Medicine, Division of Infectious Diseases, Stanford University School of Medicine, Stanford, CA 94305

Received for publication February 1, 2006. Accepted for publication June 2, 2006.

The costs of publication of this article were defrayed in part by the payment of page charges. This article must therefore be hereby marked *advertisement* in accordance with 18 U.S.C. Section 1734 solely to indicate this fact.

[1] This work was supported by Grant PO1 AI48212 from the National Institutes of Health (to E.D.M. and E.S.M.), Grant RO1 AI30363 (to E.S.M.), Medical Scientist Training Program Grant GM07365 from the National Institute of General Medical Sciences (to R.K.L.), Grant BU 1822/1-1 from the Deutsche Forschungsgemeinschaft (to T.B.), and a Walter V. and Idun Y. Berry Fellowship of Stanford University (to A.W.L.).

[2] Current address: University of Western Ontario, London, Ontario, Canada.

[3] Current address: DiscoveRx Corporation, Fremont, CA 94538.

[4] Current address: Roche Biosciences, Palo Alto, CA 94304.

[5] Address correspondence and reprint requests to Dr. Elizabeth D. Mellins, Department of Pediatrics, Stanford University School of Medicine, 269 Campus Drive, Center for Clinical Sciences Research Building, Room 2115c, Stanford, CA 94305-5164. E-mail address: mellins@stanford.edu

[6] Abbreviations used in this paper: HCMV, human CMV; LC, Langerhans cell; dpi, days postinfection; MOI, multiplicity of infection; B-LCL, B lymphoblastoid cell line; MFI, mean fluorescence intensity; DC, dendritic cell; Cat S, cathepsin S; US, unique short.

0022-1767/06/$02.00

HCMV required differentiation of cells into mature LC. At 2 days postinfection (dpi), we observed reduced levels of several cell surface molecules, including HLA-DR, HLA class I, CD86, and CD83, implying that encounter with HCMV modulates immune function of mature LC. Consistent with this prediction, infected cultures were deficient in stimulation of alloreactive T cell proliferation (19).

In our current study, we sought to further characterize effects on HLA-DR. We found that these molecules are localized away from the cell surface in both productively infected (viral Ag-positive) and exposed (viral Ag-negative) cells. Unexpectedly, we also discovered that HCMV disrupts the cytoskeletal architecture of dendrites, altering key structures implicated in Ag presentation to T cells.

Materials and Methods

Generation of CD34$^+$ progenitor-derived cell populations

G-CSF mobilized peripheral blood CD34$^+$ progenitors were purchased from BioWhittaker or obtained through the Fred Hutchinson Cancer Research Center (Seattle, WA), courtesy of Dr. S. Heimfeld. The progenitor cells were ≥90% CD34$^+$. Immature LC were derived as previously described (20, 21). To generate mature LC, purified immature LC clusters were disaggregated by repetitive pipetting and seeded in "mature LC medium," composed of X-VIVO 15 (Cambrex) containing 10% FBS, 200 ng/ml CD40L (Amgen), and 1500 IU/ml GM-CSF for 2 days. Inclusion of FBS was not necessary for either LC maturation or viral infection, but it enhanced mature LC viability during the extended periods of culture required to follow infected cells (data not shown).

Preparation of virus, infection, and LPS treatment of mature LC

HCMV strain AD169*var*ATCC was obtained from the American Type Culture Collection (ATCC). AD169*var*DE, RVAd65 (a pp65-deleted mutant virus derived from AD169*var*DE (22)), RV798 (a US2-US11 deletion mutant virus derived from AD169*var*ATCC (23)), and TB40/E were gifts from M. Mach (University of Erlangen-Nürnberg, Erlangen, Germany), B. Plachter (University of Mainz, Mainz, Germany), T. Jones (Wyeth-Ayerst Research, Pearl River, NY), and C. Sinzger, (University of Tübingen, Tübingen, Germany), respectively. Virus strains were propagated at a multiplicity of infection (MOI) of 0.01 in confluent human foreskin fibroblasts and purified as described (24), then briefly sonicated and stored at −80°C in 200-μl aliquots. Fibroblasts were *Mycoplasma* negative upon multiple testing (data not shown). Virus titers were determined by plaque assay on monolayers of human foreskin fibroblasts in 12-well tissue culture plates. For infection of mature LC, 2×10^5 cells/well in 48-well plates were infected at an MOI of 100 PFU/cell for 1–2 h; titrations from MOI of 10–200 showed maximal IE1/IE2 expression (~70% IE1/IE2$^+$) in mature LC infected at an MOI of 50 or greater (19). To minimize well-to-well variability and to exclude adherent cells from the cultures, mature LC were gently harvested, pooled, and replated into new tissue culture plates at least 2 h before infection. Virus stocks were diluted in mature LC culture medium and filtered through a 0.45-μm filter immediately before use; this step did not reduce infectivity (data not shown). The culture medium from each well was removed and replaced with 200–300 μl of virus inoculum. After adsorption for 2 h at 37°C, the virus-containing medium was removed and replaced with 300 μl/well of mature LC medium containing FBS, CD40L, and GM-CSF. Mock-infected cells were treated in the same manner without addition of virus.

For some experiments, an infection protocol was modified to reduce the cell loss occurring during culture medium removal. In the modified procedure, mature LC were harvested into 15-ml tubes, washed twice with serum-free medium, resuspended in viral inoculum, centrifuged at 1300 rpm for 10 min, and incubated at 37°C for 1 h. Following incubation, cells were washed with serum-containing medium, resuspended in mature LC medium as described, and replated. Experiments with both infection protocols showed comparable levels of IE1/IE2 expression and HLA-DR reduction, but increased cell retention following the modified protocol (data not shown).

For UV inactivation, TB40/E stocks were diluted in DMEM to a final concentration of 7×10^8 PFU/ml, distributed into a 12-well plate (150 μm/well), and irradiated for 4.5 min at ~4 cm away from an 1800 StrataLinker UV lamp (Stratagene). Inactivated virus was kept for 2 h in the dark at room temperature and diluted 10-fold in mature LC medium before use. The efficacy of inactivation was tested by immunofluorescence staining of human foreskin fibroblasts infected with the irradiated virus at a calculated MOI of 10 using a FITC-conjugated anti-IE1/IE2 mAb (clone 8B1.2; Chemicon International) or an anti-pp65 (ppUL83) mAb (clone 28-19; W. Britt, University of Alabama, Birmingham, AL) followed by a Texas Red-conjugated anti-mouse Ab. UV irradiation completely abrogated IE1/IE2 expression, whereas anti-pp65 staining of cells infected with UV-irradiated and nonirradiated virus stocks were comparable (data not shown). For LPS treatment of cells, a crude LPS preparation from *Escherichia coli* (Sigma-Aldrich) containing both LPS and lipoprotein (i.e., TLR4 and TLR2 ligands (25)) was added to cell culture at 0.5 μg/ml.

Flow cytometry

Two-color FACS analysis was performed as described previously (19). For three-color analysis, cells were surface stained with combinations of anti-CD83 PE and anti-DR PerCP, or anti-CD83 allophycocyanin and anti-DR PE mAbs, followed by intracellular anti-IE1/IE2 FITC (clone 8B1.2; Chemicon International). Ab to CD83 (PE; clone HB15e), HLA-DR (PerCP, clone L243) (26), and appropriate isotype controls were obtained from BD Biosciences. Ab against HLA-DR (FITC or PE, clone TU36), total HLA class I (FITC or PE, clone TU149), CD83 (allophycocyanin, clone HB15e), and respective isotype controls were purchased from Caltag Laboratories. All procedures were conducted at 4°C. For determination of surface or total HLA-DR levels, the anti-HLA-DR Ab was added to cells before or following fixation and permeabilization, respectively.

For analysis of two-color samples, mature LC were identified within mock-infected cultures by gating on all CD83 PE-positive cells and displaying their forward and side light scatter profile, and drawing another gate that excluded dead or small cells and included >70% of CD83-positive cells ("CD83$^+$ gate"). The CD83$^+$ gate was then transferred to mock-infected samples stained with anti-HLA class I PE or anti-HLA-DR PE. To identify infected mature LC, a gate was drawn to include all IE1/IE2 FITC-positive cells, displaying the forward and side light scatter profile of these cells, superimposing the CD83$^+$ profile gate discussed, and positioning this gate to include at least 70% of IE1/IE2$^+$ cells. For three-color analysis, each individual sample was gated on CD83$^+$ and IE1/IE2+ cells for mock- and HCMV-infected mature LC, respectively. Events were acquired on a FACScan or a FACSCalibur (BD Biosciences) and analyzed using FlowJo software (Tree Star).

Transwell culture of mature LC

Mature LC were infected with HCMV or mock-treated as described and transferred to sterile polycarbonate membrane Transwell plates (Costar). The Transwells were situated above the wells harvested for FACS analysis, allowing for gravity-mediated exchange of fluid from the Transwell to the assayed well. Cultures were incubated at 37°C for an additional 2 days before collection and flow cytometry analysis.

Quantification of total cellular HLA-DR by ELISA

Anti-HLA-DR mAb (L243) was immobilized on ELISA plates. The plates were incubated with 2% BSA in PBS for 2 h at 37°C to block nonspecific binding of cell lysate proteins, and washed three times with PBS-T (PBS plus 0.05% Tween 20). Titrated amounts of cell lysate from control B lymphoblastoid cell lines (B-LCL), 8.1.6 (DR-positive), and 6.1.6 (DR-negative) (27) and from differently treated mature LC were prepared in PBS plus 0.01% IGEPAL and incubated with the immobilized Ab for 1 h at 37°C. After washing with PBS-T, the plates were incubated with CHAMP, an anti-DR rabbit antisera, at a 1/5000 dilution for 1 h at 37°C. After washing three times with PBS-T, the plates were incubated with an anti-rabbit peroxidase-labeled secondary Ab (1/1000) for 1 h at 37°C. After washing, the plates were developed using the colorimetric substrate ABTS, and absorbance at 405 nm was measured with a 96-well plate reader Wallac 1420 workstation.

Fluorometric measurement of cathepsin S activity

Catalytic activity of cathepsin S (Cat S) was determined fluorometrically as described elsewhere (28). Liberated fluorescence (excitation 380 nm, emission 460 nm) was measured every 5 min with a Gemini XS multiwell fluorometer (Molecular Devices).

Western blot and SDS stability assay

The SDS stability assay was performed as described previously (29). Briefly, aliquots of Nonidet P-40-solubilized cell lysates were diluted 1/1 in 0.4% SDS-containing Laemmli buffer and incubated at 4°C for 30 min or boiled for 10 min, before analysis by SDS-PAGE. After transfer to polyvinylidene difluoride membranes, immunoblotting was performed with mAb HB10A, which recognizes DRβ with a preference for DR$\alpha\beta$

heterodimers, or with mAb DA6.147, which recognizes DR$\alpha\beta$ heterodimers with a preference for DRα monomers, followed by HRP-conjugated goat anti-mouse IgG, and an ECL substrate (Renaissance; DuPont/NEN). B-LCL 8.1.6 was used as a positive control and DM-negative B-LCL 9.5.3 was used as a negative control for dimer stability assays (27).

Endocytosis of biotin-labeled HLA-DR

Immature LC, mock-treated mature LC, and HCMV-infected mature LC were harvested as described and washed with PBS. Cells were resuspended in PBS plus 0.5% BSA (FACS medium) for 15 min at room temperature, pelleted, and then incubated with saturating amounts of biotin-conjugated anti-HLA-DR (clone L243; BD Biosciences) for 5 min at room temperature. Cells were washed three times with excess volumes of PBS, resuspended in prewarmed FACS medium, and incubated at 37°C. At 0, 10, 20, 40, and 80 min, aliquots of cells were stained with saturating amounts of Streptavidin-PerCP conjugate (BD Biosciences) for 30 min at room temperature. Cells were washed with PBS and analyzed on the flow cytometer. The mean fluorescence intensity (MFI) for anti-HLA-DR staining was determined for each cell type at each time point and normalized to the time ($t = 0$) value. Percentage of HLA-DR recycled is $100 - [(\text{MFI of time } t \text{ of DR staining})/(\text{MFI of DR staining at time } t = 0)] \times 100$. Control groups of cells stained with streptavidin conjugate only had fluorescence levels comparable to unstained cells, and other control groups incubated on ice or in azide-containing medium (0.1%) endocytosed <10% of HLA-DR over the same time period (data not shown).

Immunofluorescence analysis and live cell microscopy

For IE1/IE2 and HLA-DR double staining, cytospin preparations were treated as described previously (19), stained with an anti-HLA-DR mAb (clone L243), and mounted with FluoroGuard Antifade Reagent (Bio-Rad). Epifluorescence microscopy images were collected at room temperature on an epifluorescence microscope (model BX60; Olympus) using a Hamamatsu ORCA-100 digital camera with Image Pro Plus 4.0 software (Media Cybernetics). Digitized images were stored, electronically colorized using Image Pro Plus 4.0 software and then overlaid using Adobe Photoshop software for evaluation of two-color experiments. Confocal microscopy images were collected at room temperature on a confocal laser scanning microscope (model MRC1024; Bio-Rad) using LaserSharp software (Bio-Rad). Phase contrast micrographs of live cells were collected at room temperature on a Nikon Eclipse TE300/200 inverted microscope using a Hamamatsu ORCA-100 digital camera with Image Pro Plus 4.0 software (Media Cybernetics). Luminosity and contrast were adjusted using Adobe Photoshop software (Adobe Systems).

Immunofluorescence for cytoskeletal elements

LPS-treated, mock-infected, and HCMV-infected mature LC were allowed to settle onto poly-D-lysine-coated microscope chambers (Biocoat; BD Biosciences) overnight at 37°C and were immunostained as previously described (30). In brief, cells were rinsed in PBS with 1 mM $MgCl_2$ and 1 mM EGTA, fixed with ice cold methanol at −20°C for 5 min, and incubated in 0.1% Triton X-100 in PBS with 1 mM $MgCl_2$ and EGTA for 30 s. Cells were then rinsed three times with PBS with 1 mM $MgCl_2$ and EGTA, blocked with 0.2% BSA in PBS with 1 mM $MgCl_2$ and EGTA, and stained for tubulin using rat mAb (1/200 dilution, clone YL 1/2; Accurate Chemical and Scientific), and anti-rat Rhodamine Red-X secondary Ab (1/200 dilution; Jackson ImmunoResearch Laboratories) or stained for fascin, using mouse mAb 55K2 (1/323 dilution; Chemicon International), and an anti-mouse Rhodamine Red-X secondary Ab (1/200 dilution; Jackson ImmunoResearch Laboratories). IE1/IE2-FITC mouse mAb 8B1.2 (Chemicon International) was used at a dilution of 1/800. Apoptotic cells were detected with Annexin V-FITC-conjugated Ab (ApoAlert; BD Biosciences) before fixation. All slides were mounted in Vectashield (Vector Laboratories).

Cells were imaged using a Zeiss Axioplan microscope with a Zeiss Plan-Neofluar ×100/1.3 oil objective. Images were recorded with a Zeiss MRm camera using AxioVision 3.1.2.1 acquisition software. Images were captured without overexposure. Exposure times in the FITC channel for IE1/IE2 were kept constant, to allow for comparison between IE1/IE2$^+$ and IE1/IE2$^-$ cells. Brightness and contrast were adjusted for the tubulin and fascin images to highlight structures at the cell periphery. IE1/IE2 images were not adjusted for brightness and contrast. Colors were arbitrarily assigned as green for tubulin and fascin, and red for IE1/IE2. Images were prepared and arranged using Adobe Photoshop, Adobe Illustrator (Adobe Systems), and ImageJ software (NIH Image software). Quantification of cells was performed manually, by visualization of nine different fields of each slide.

In vitro Transwell chemotaxis

Methods were adapted from Zabel et al. (31). Briefly, chemotaxis through a 5-μm pore Transwell insert (Costar) in response to chemokine was compared for mock-infected and TB40/E-infected mature LC (MOI = 100, 3 dpi). Chemokine medium consisted of X-VIVO plus 10% FBS, supplemented with 1–100 nM CCL19, CCL21, CXCL12, or a mixture of all three chemokines (R&D Systems), and was added to the bottom well in a 600-μl volume. A total of 2–5 × 10^5 mature LC was added to the top Transwell in a 100-μl volume and incubated for 4 h at 37°C. The inserts were removed, and the cells that had migrated through the filter to the lower chamber were stained (CD83-allophycocyanin and IE1/IE2-FITC) and counted by flow cytometry. An equivalent number of beads (CompBeads negative control; BD Biosciences) were added to each tube to normalize the cell count. The number of CD83$^+$ cells plus IE1/IE2$^+$ cells counted in 60 s was designated as the mature LC migration output. The results are reported as a percentage of input migration.

Results

Timing of HCMV modulation of surface expression of HLA-DR, HLA class I, and CD83 in mature LC

We previously observed reductions in surface HLA-DR, HLA class I, and CD83, a DC maturation marker with immunomodulatory activity (32) on mature LC at 2 dpi (19). To extend these studies, we determined the impact of HCMV on mature LC cultures over a 3-day time course following infection. After exposure to endothelial-tropic strain TB40/E (MOI = 100), IE1/IE2$^+$ mature LC displayed progressively larger reductions in surface HLA-DR, whereas mock-infected mature LC increase surface HLA-DR over the same time period (Fig. 1*A*). IE1/IE2$^+$ mature LC exhibited lower MFI of HLA-DR at 2 and 3 dpi ($n = 8$), and of MHC class I at 3 dpi ($n = 4$), and CD83 at 1, 2, and 3 dpi ($n = 7$) compared with mock-infected cells ($p < 0.05$; Fig. 1*B*). Analysis of other surface markers, such as CD40, showed no significant differences between mock-infected and IE1/IE2$^+$ cells over 1–3 dpi (p = NS, $n = 3$; Fig. 1*B*). Thus, selected DC surface molecules, including HLA-DR, are reduced in IE1/IE2$^+$ cells.

Exposure to HCMV modulates surface HLA-DR expression in IE1/IE2$^-$ mature LC

To determine whether viral gene expression was required for modulation of cell surface proteins, we compared levels of HLA-DR, HLA class I, and CD83 in IE1/IE2$^+$ and IE1/IE2$^-$ mature LC. We found that surface HLA-DR was reduced to a similar degree in both populations (MFI of 355 and 357) compared with mock (MFI of 659) (Fig. 2*A*, *left*). In contrast, the IE1/IE2$^-$ cells modestly increased surface HLA class I (Fig. 2*A*, *center*), and expressed CD83 at levels comparable to mock-infected cells (Fig. 2*A*, *right*). Together, these results suggest that distinct mechanisms regulate HLA-DR, HLA class I, and CD83 in HCMV-exposed mature LC cultures.

To test whether a soluble factor produced by IE1/IE2$^+$ mature LC was sufficient to inhibit surface HLA-DR expression on IE1/IE2$^-$ mature LC, we measured the effects of medium from HCMV-exposed mature LC on unexposed cultures, using a Transwell system. We observed reduced HLA-DR in IE1/IE2$^+$ mature LC that had direct contact with virus, but not in cells exposed to conditioned medium (Fig. 2*B*).

We then considered the possibility that exposure to virus particles was sufficient to influence surface HLA-DR levels. We measured expression of surface HLA-DR in cells exposed to medium (mock), TB40/E, UV-treated medium (UV-mock), and UV-inactivated TB40/E. At 2 and 3 dpi, cells exposed to either TB40/E or UV-inactivated TB40/E exhibited reduced surface HLA-DR levels (data shown for 3 dpi only) (Fig. 2*C*). As additional controls, we

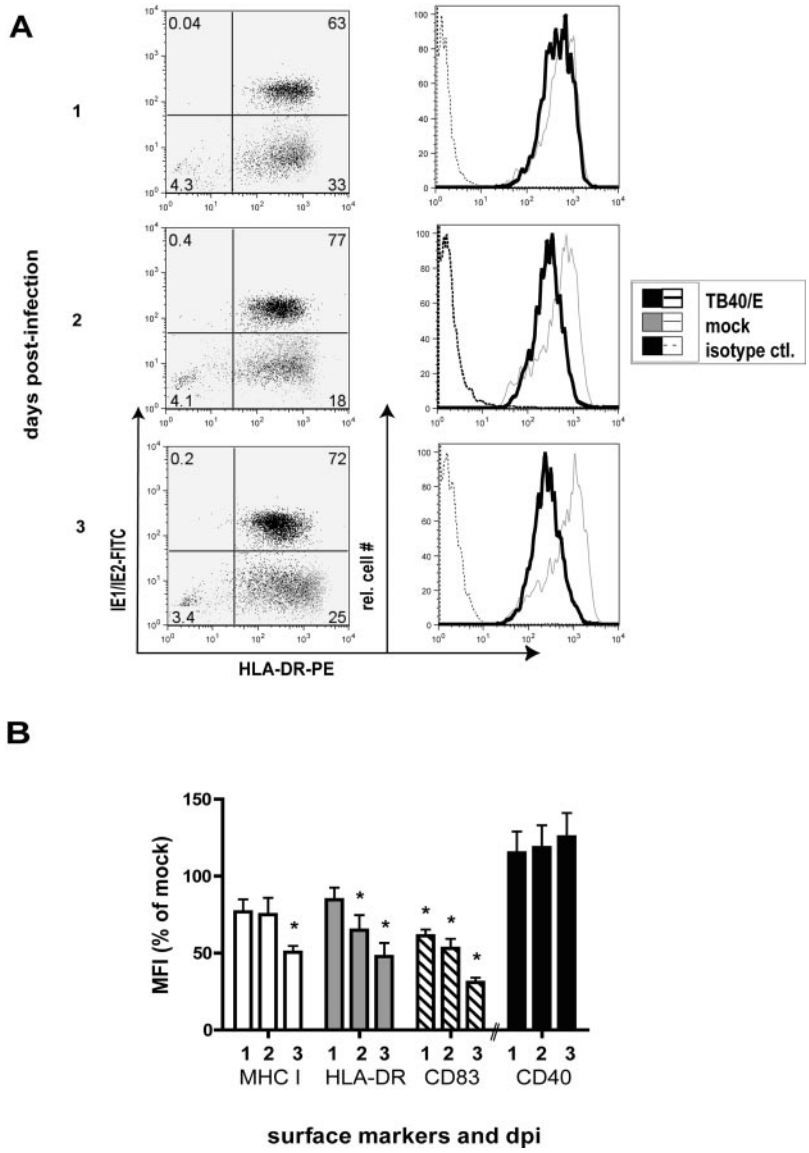

FIGURE 1. HCMV infection of mature LC leads to a sustained reduction of HLA-DR, MHC class I, and CD83 levels, compared with mock-infected cells. *A*, Overlays of dot plot (*left*) and histogram (*right*) analyses showing surface HLA-DR levels in mock-infected (gray, thin line histogram) and TB40/E-infected (MOI = 100) (black, thick line histogram) mature LC cultures at 1–3 dpi. Thick black lined histogram represents IE1/IE2$^+$ events only. Cells are stained with PE-conjugated anti-HLA-DR (*x*-axis of dot plots) and FITC-conjugated anti-IE1/IE2 mAb (*y*-axis). Percentage of total events in each quadrant is shown for HCMV-exposed mature LC cultures only. One representative of eight experiments, from three donors, is shown. *B*, Summary of surface MHC class I ($n = 4$), HLA-DR ($n = 8$), and CD83 ($n = 7$) levels in infected mature LC as a percentage of levels in mock-infected cells. Average values with SE bars are shown. ∗, Statistically significant difference from mock-treated cells ($p < 0.05$ by one-sample *t* test). Data are from three donors. Surface CD40 levels were also evaluated in three separate experiments over the same time course. Similar results were obtained in experiments at 2 dpi, when staining with Abs to all four surface molecules was done in parallel (19).

treated mature LC with LPS (0.5 μg/ml) or live *Bordetella pertussis* (MOI = 100) and observed minimal changes in surface HLA-DR levels with either stimulus (average ratio of LPS to mock HLA-DR at MFI = 1.020, p was not significant ($n = 4$); average *B. pertussis*/mock HLA-DR at MFI = 1.002). Thus, exposure to HCMV particles reduces surface levels of HLA-DR molecules on mature LC, and this is not a general feature of all microbial stimuli.

HCMV unique short US2-US11 region is not required for modulation of surface HLA-DR in mature LC

We were interested in testing particular HCMV components to determine whether they play a role in modulation of HLA-DR surface levels. There are no well-characterized mutants of TB40/E. We therefore used mutants of a laboratory-adapted HCMV strain, AD169*var*ATCC (AD169). Despite large deletions in its genome (33), AD169 can infect nonfibroblast cell types, including mature LC, although infection is not as efficient as with TB40/E (19). To evaluate the ability of AD169 to diminish surface HLA-DR on mature LC, we compared IE1/IE2$^+$CD83^{low} cells in cultures infected with AD169 and TB40/E. We focused on CD83^{low} cells because these are the cells in which HLA-DR is modulated (data not shown), and their abundance differs in IE1/IE2$^+$ cells infected with TB40/E (85%, CD83^{low}) and AD169 (45%, CD83^{low}) (Fig. 3*A*). Following exposure to either TB40/E or AD169, IE1/IE2$^+$CD83^{low} cells reduced surface HLA-DR equivalently (Fig. 3*B*).

Next, we examined whether the AD169-derived mutant virus RV798, lacking the unique short (US) genomic region encompassing US2-US11, was able to mediate HLA-DR inhibition. Products of the US2 and US3 genes have been implicated in altering levels of HLA-DR in transfected non-DC types (15, 34) and negatively affect HLA class I levels in several cell types (35). AD169 and RV798 did not differ in their capacity to infect mature LC cells based on the frequency of IE1/IE2$^+$ cells (data not shown). In four experiments, both wild-type AD169 and RV798 significantly reduced surface HLA-DR (MFI ratio of infected/mock = 0.596 and 0.580, respectively, $p < 0.003$ for both) (Fig. 3*C*). In contrast, reduced surface HLA class I was seen only following wild-type virus infection (AD169/mock ratio = 0.624, $p < 0.01$; RV798/mock ratio = 1.31, p = NS) (Fig. 3*C*). Although the HCMV proteins encoded by the US2-US11 region modulate HLA class I levels in mature LC, they do not have a discernible effect on surface HLA-DR levels in infected mature LC during the time frame examined.

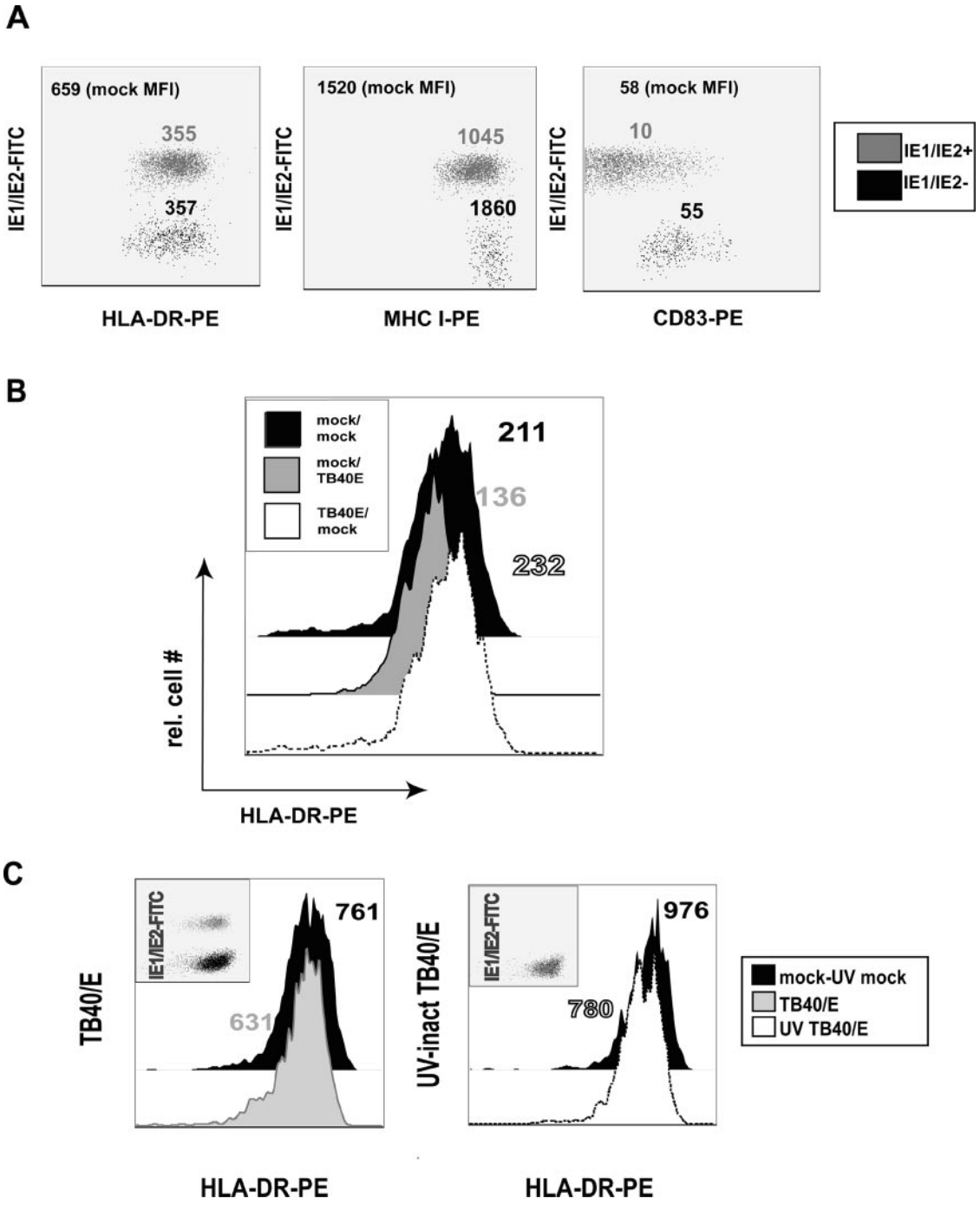

FIGURE 2. HLA-DR is decreased in IE1/IE2$^-$ mature LC exposed to live and UV-inactivated HCMV but not following exposure to medium of HCMV-infected mature LC. *A*, Dot plot analyses of anti-HLA-DR, anti-MHC class I, or anti-CD83 vs anti-IE1/IE2 in mature LC exposed to TB40/E. MFI values minus isotype control value for each Ab using mock-infected cultures are shown (*upper left-hand corner*) for comparison to IE1/IE2$^+$ (gray) and IE1/IE2$^-$ (black) populations. One representative experiment of three is shown. Data are from three donors. Reduced surface HLA-DR in IE1/IE2$^+$ and IE1/IE2$^-$ cells was observed in 15/15 donors (binomial test, $p < 0.0001$), although the percentage decrease varied (15–60%) from experiment to experiment. The reduction in surface HLA-DR was not related to induction of cell death by apoptosis (data not shown). *B*, Analyses of surface HLA-DR levels on mock-infected, conditioned medium-exposed, and HCMV-infected mature LC. Mock or HCMV-infected mature LC were transferred to polycarbonate membrane-separated (0.1-μm pore size) Transwells (upper chamber) and incubated for an additional 2 days in mature LC medium. Cells in lower chamber were assessed by flow cytometry; mock-treated with mock-treated Transwell (mock/mock, black), TB40/E-infected with mock-treated Transwell (mock/TB40E, gray), and mock-treated with TB40/E-infected Transwell (TB40E/mock, white). Mock-infected cells, including those exposed to infected medium via the Transwell, had <1% IE1/IE2$^+$ cells (data not shown). MFI of anti-HLA-DR staining, minus isotype control, are shown; data are from one representative experiment of two and from four donors. *C*, Histogram and dot plot (*inset*) analyses of surface HLA-DR levels on mock (black), TB40/E-infected (gray), UV-treated medium (black), and UV-inactivated TB40/E-exposed (white) mature LC at 3 dpi. Cells exposed to UV-inactivated TB40/E had <1% IE1/IE2$^+$ cells (data not shown). MFI values of anti-HLA-DR PE staining, minus isotype control Ab are shown. Data are from one representative experiment of four.

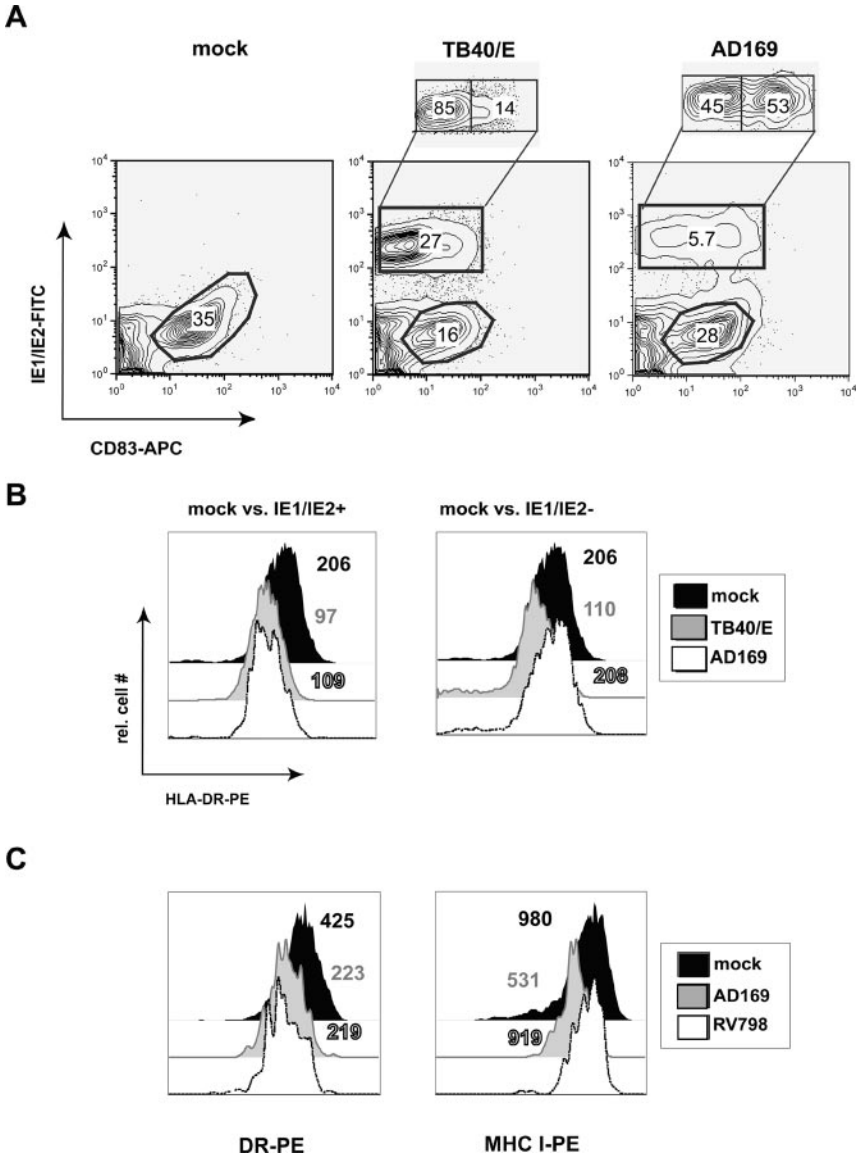

FIGURE 3. Infection of mature LC with endothelial-tropic, fibroblast-adapted, and mutant HCMV. *A* and *B*, Flow cytometric analysis of uninfected (mock), TB40/E-infected, and AD169-infected mature LC at 2 dpi. Cells were infected at MOI = 100. Cells were stained with anti-HLA-DR PE, anti-CD83 allophycocyanin, and anti-IE1/IE2 FITC. *A*, Contour plots of CD83 vs IE1/IE2 staining. *Inset*, gates, and percentages of IE1/IE2^{+}CD83^{low} and IE1/IE2^{+}CD83^{high} subsets of all IE1/IE2^{+} cells are shown for TB40/E and AD169-exposed cells. *B*, Histogram analysis of surface HLA-DR levels in differently treated mature LC. The mock-infected sample was gated on CD83^{+} cells and the HCMV-infected samples were gated on IE1/IE2^{+}CD83^{low} and IE1/IE2^{-}CD83^{+} cells, as shown in *A*. MFI values of anti-HLA-DR staining (isotype control value subtracted) for each subpopulation are shown in the same shading as the corresponding histogram. One representative experiment of four is shown. *C*, HLA-DR and MHC class I surface levels in uninfected (mock), AD169 (parental wild-type), and RV798 (US2-US11 deletion mutant) infected mature LC at 3 dpi. Cells were infected at MOI = 20. Histograms represent IE1/IE2^{-} CD83^{+} cells from mock cultures and IE1/IE2^{+} CD83^{low} cells from virally infected cultures. MFI values, minus isotype control value, for anti-HLA-DR and anti-MHC class I staining are shown in the same shading as the corresponding histogram. One of three independent experiments with similar results is shown.

Total cellular HLA-DR levels remain unchanged in HCMV-infected mature LC

Reduction in cell surface HLA-DR levels could reflect either diminished levels of total cellular HLA-DR or altered localization to intracellular compartments. To distinguish between these possibilities, we measured total cellular levels of HLA-DR in mock-treated and HCMV-infected mature LC by sandwich ELISA. As shown in Fig. 4, lysates from mock and infected mature LC cultures titrated across a range of protein concentrations (from 1.25 to 10 μg) had comparable levels of HLA-DR protein; lysates from control

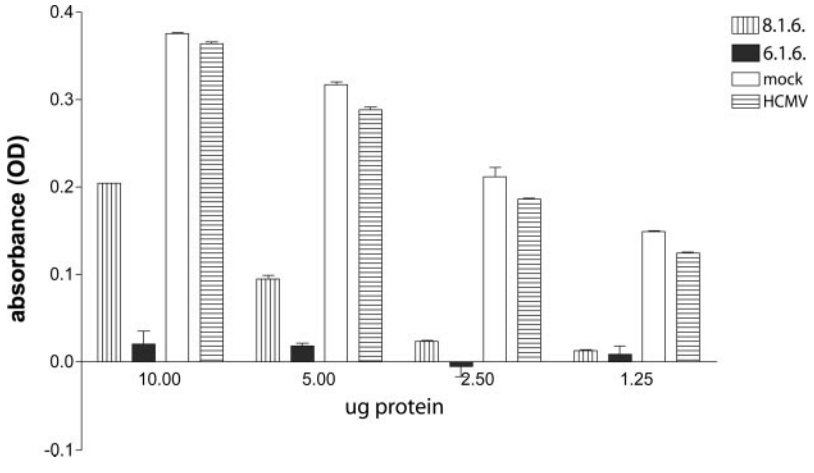

FIGURE 4. Total HLA-DR levels are not reduced in mature LC following exposure to HCMV. Titrated total cellular protein lysates from HLA-DR-positive (8.1.6.), HLA-DR-negative (6.1.6.), control B-LCL, mock-treated, and TB40/E-infected (MOI = 100, 2 dpi) mature LC were assayed for total HLA-DR by sandwich ELISA. Mean value shown with range from duplicate wells. Data are from one donor of four, each tested in two experiments with similar results.

HLA-DR positive (8.1.6.) and negative (6.1.6.) B-LCL exhibited obvious differences in DR levels. To confirm these results with a different method, we also measured surface and total DR levels in mock and infected mature LC by flow cytometry. HCMV-infected mature LC had decreased levels of surface, but not total, HLA-DR (data not shown). The combination of reduced surface and unchanged total HLA-DR in HCMV-infected mature LC indicate that HLA-DR localization is altered in infected cells.

Cat S levels and activity remain unchanged in HCMV-infected mature LC

We considered the possibility that intracellular accumulation of HLA-DR protein was achieved through effects on Cat S levels and/or activity. Nascent HLA class II molecules in the endoplasmic reticulum associate with the chaperone, invariant chain, and are guided to endosomal compartments by a targeting motif in the invariant chain cytoplasmic tail. Expression of HLA class II molecules at the cell surface does not occur until invariant chain is cleaved by a cathepsin, with Cat S being the strongest candidate cathepsin in DCs (36). A comparison of Cat S levels in lysates of mock- and TB40/E-infected mature LC at 2 dpi showed no significant differences by immunoblot analysis (Fig. 5*A*). The activity of Cat S also was very similar in mock- and HCMV-infected cells, as judged by proteolysis of a fluorogenic substrate (Fig. 5*B*). Thus, altered localization of HLA-DR in HCMV-infected mature LC cultures does not appear to be due to modulation of Cat S.

Levels of SDS-stable HLA-DR dimers remain unchanged in HCMV-infected mature LC

HLA class II $\alpha\beta$ dimers that are associated with invariant chain, with their intermediates generated by proteolysis, or with low affinity peptides, generally remain susceptible to in vitro dissociation by SDS detergent without boiling. In contrast, after peptide-loading and editing by HLA-DM in late endosomal compartments, "mature" class II molecules acquire an SDS stable phenotype (37, 38). To localize HLA-DR molecules in HCMV-exposed mature LC, we determined whether the ratio of immature forms to mature, peptide-loaded forms of HLA-DR was altered following viral exposure, using SDS stability as an assay. We compared HLA-DR molecules in lysates from mock-infected with TB40/E-infected mature LC cultures and found that SDS-stable dimers represented a comparable, majority proportion of the total HLA-DR molecules in both cultures (Fig. 5*C*). These results indicate that HCMV-infected mature LC support HLA-DR assembly/transport and loading of peptide, but accumulate mature, peptide-loaded molecules intracellularly.

Endocytosis of surface HLA-DR in infected mature LC is not increased

Intracellular sequestration of mature HLA-DR in HCMV-infected cells could result from either a block in egress from the peptide-loading compartments or an increase in recycling of surface molecules. To determine whether HCMV infection increases recycling of surface HLA-DR, we compared endocytosis of biotin-labeled HLA-DR in mock-infected and TB40/E-infected mature LC, using a flow cytometry-based assay (see *Materials and Methods*). As a control, we measured endocytosis in immature LC, which are known into have higher rates of endocytosis compared with mature LC (39). We found no evidence for increased recycling of biotin-labeled HLA-DR in HCMV-infected vs mock-treated mature LC over the assayed time period (Fig. 6). Indeed, we observed a trend

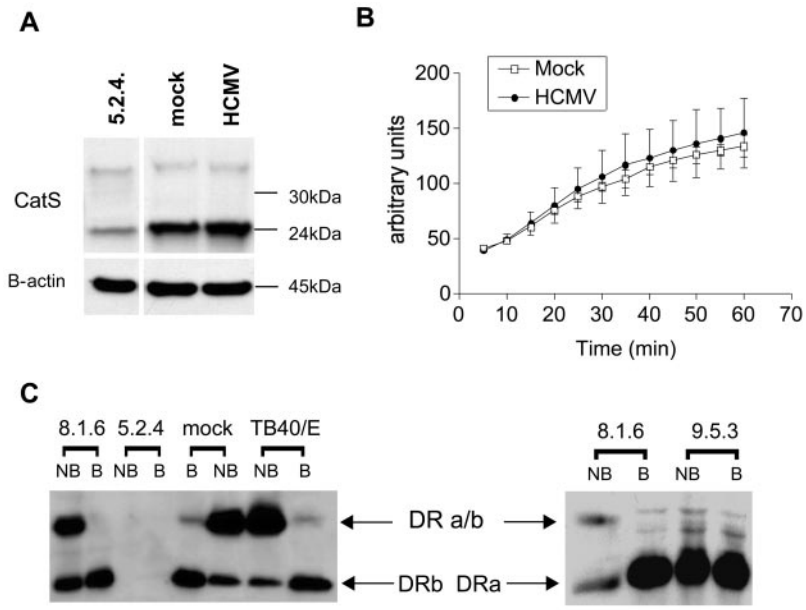

FIGURE 5. HCMV infection does not significantly affect Cat S levels, activity, or the proportion of SDS-stable HLA-DR dimers. *A*, Western blot analysis of Cat S. Whole cell lysate was prepared from mock-treated, TB40/E-infected (MOI = 100, 2 dpi) mature LC, and HLA-DR-negative B-LCL (5.2.4). Protein (5 μg) was loaded from each cell lysate. The specificity of the anti-Cat S Ab was confirmed with recombinant Cat S (data not shown). Both the proform (40 kDa) as well as the active Cat S polypeptide (24 kDa) were detected. β-actin served as a loading control. *B*, Cat S activity from cell lysate (0.4 μg) of mock-treated and TB40/E-infected mature LC was measured using the fluorogenic substrate Z-FR-AMC and the fluorescence (emission 460 nM) was quantitated in arbitrary units. *C*, Western blot analysis of HLA-DR $\alpha\beta$ dimer and β monomer (*left*) from nonboiled (NB) and boiled (B) whole cell lysates of 8.1.6, 5.2.4, mock-infected, and TB40/E-infected mature LC at 2 dpi is shown. Protein (15 μg) from each lysate was analyzed on a 12% SDS-PAGE gel under nonreducing conditions. The lysates were stained with HB10A, an anti-DRβ mAb with a preference for the dimeric form of HLA-DR. *C*, As a control for the detection of reduced SDS stability, lysates from 8.1.6 and HLA-DM-negative B-LCL (9.5.3) were stained with DA6.147 (*right*), a mAb with a preference for the monomeric form of HLA-DRα. These results are representative of four independent experiments.

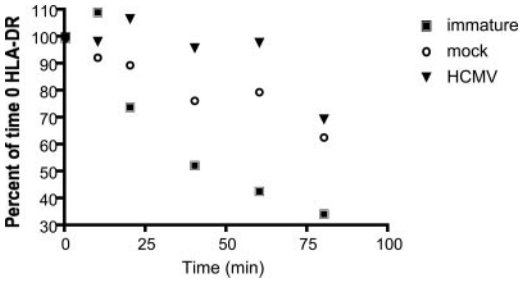

FIGURE 6. Endocytosis of HLA-DR is not increased following exposure to HCMV. Immature, mock, and HCMV-infected LC were incubated with biotinylated anti-HLA-DR (L243), washed extensively, and incubated at 37°C for up to 80 min. The amount of biotinylated HLA-DR remaining at the cell surface was then determined by FACS analysis, using a streptavidin conjugate. One representative of three experiments is shown.

toward slightly reduced endocytosis of HLA-DR in HCMV-infected vs mock mature LC, although the difference was not statistically significant over three experiments. The lack of evidence for increased recycling argues that the altered localization of HLA-DR in HCMV-infected mature LC is the result of a block in egress from peptide-loading compartments.

Distribution of HLA-DR in HCMV-infected mature LC by immunofluorescence microscopy

We complemented our flow cytometry and SDS stability studies by immunofluorescence microscopy to visualize the altered localization of HLA-DR in HCMV-infected mature LC. Cytospin preparations of mock- and TB40/E-infected mature LC were stained for IE1/IE2 Ag and for HLA-DR at 2 dpi. Low magnification (×400) images revealed the majority of mock-infected cells exhibited HLA-DR in a ring-like distribution typical of mature DCs (40), with concentrations at the cell surface and in a perinuclear region (Fig. 7, *A* and *C*). Although viral Ag-negative cells showed a staining pattern similar to mock-infected cells (Fig. 7*B*, far right, compare the IE1/IE2$^-$ cell with *A*), IE1/IE2$^+$ cells showed a spectrum of HLA-DR distribution patterns (Fig. 7*B*, low magnification), including small perinuclear clusters (Fig. 7, *D* and *B,* asterisk), bulky clumps (Fig. 7, *E* and *B,* arrowhead), and diffuse, low intensity staining (Fig. 7, *F* and *B,* arrow). Moreover, costaining with a mAb specific for the lysosome-associated membrane protein-1 revealed only partial colocalization of HLA-DR and lysosome-associated membrane protein-1 in IE1/IE2$^+$ cells (data not shown). In contrast to the heterogeneity in cytoplasmic HLA-DR distribution, a uniform finding in IE1/IE2$^+$ mature LC was decreased intensity of HLA-DR staining at the cell surface, notably in the hair-like dendritic projections, (Fig. 7*C*, cf to *D–F*). Modifications in the distribution of HLA-DR were specific for infected cultures, as cells treated with dose LPS did not show similar changes (data not shown).

To gain additional insights into the distribution of HLA-DR in infected cells, we performed confocal laser scanning microscopy analyses of TB40/E-infected mature LC. Fig. 7*G* shows a representative image of HLA-DR localization in IE1/IE2$^+$ and IE1/IE2$^-$ cells. The majority of HLA-DR appeared to localize away from the cell surface in IE1/IE2$^+$ mature LC, based on reduced fluorescence intensity at the cell periphery and an absence of HLA-DR-positive cell surface dendrites characteristic of mature LC.

Loss of dendrite architecture in HCMV-infected mature LC

To determine whether the loss of HLA-DR that normally outlines the surface of dendrites was due to altered distribution of HLA-DR

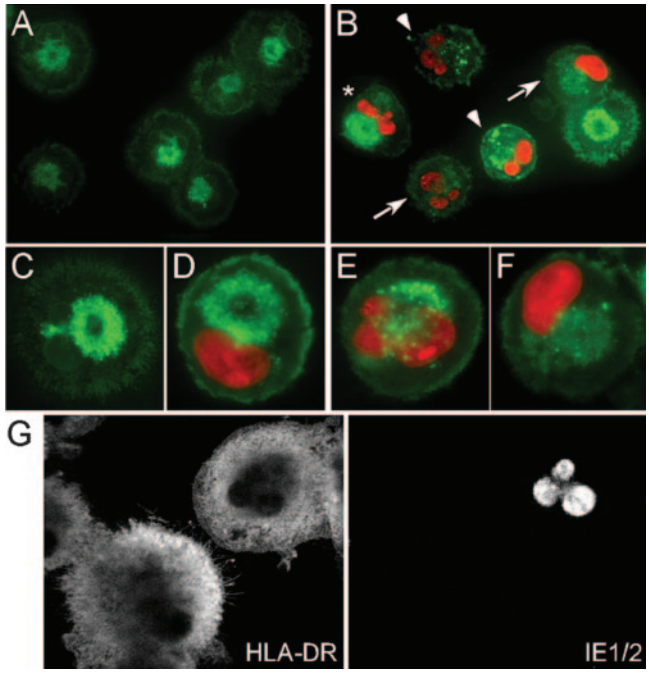

FIGURE 7. HCMV modifies HLA-DR localization in infected mature LC. *A–F*, Cytospin preparations of mock- or TB40/E-infected (MOI = 100, 2 dpi) mature LC stained with mAb against HLA-DR (green), and IE1/IE2 mAb (red). *A* and *C*, Mock-infected mature LC at low (×400) (*A*) and high (×1000) (*C*) magnification. Note that the signal seen toward the center of the cell represents a summation of the fluorescent signal for the entire thickness of the cell. *B* and *D–F*, TB40/E-infected mature LC at low (×400) (*B*) and high (×1000) (*D–F*) magnification. The asterisk, arrowheads, and arrows point at IE1/IE2$^+$ cells displaying "clustered," "clumped," and "diffuse" DR phenotypes, respectively. *G*, Confocal microscopy images of TB40/E-infected mature LC at 2 dpi stained with mAb against HLA-DR (*left*) and IE1/IE2 (*right*). Original magnification, ×600.

or to the loss of the entire dendritic structure, we compared the morphology of mock-treated, TB40/E-infected, and LPS-treated mature LC cultures by phase-contrast microscopy. Strikingly, although characteristic clusters of mature LC in mock-infected and LPS-treated cells displayed numerous dendritic veils, rounded cells lacking dendrites were observed at 2 dpi (data not shown) and 3 dpi in the TB40/E-infected cultures (Fig. 8*A*). Our results argue that the apparent loss of HLA-DR positive dendrites seen on immunofluorescence and confocal microscopy of virus-infected cells was in fact due to loss of entire dendritic projections.

To further explore how HCMV alters the structure of infected mature LC, we investigated whether viral infection affected microtubules, recently shown in live-imaging studies to be important for formation and extension of MHC class II-positive tubules in DC (41). As shown in Fig. 8*B*, double immunofluorescence staining for α-tubulin and IE1/IE2 expression revealed that mock and LPS-treated mature LC possess numerous long, thin, tubulin-positive dendrites beyond the cell body. In contrast, HCMV-exposed mature LC had reduced tubulin extensions (both in number and in length), with marked loss of dendrites occurring in the IE1/IE2$^+$ cells (compare IE1/IE2$^-$ cell vs IE1/IE2$^+$ cell in center column of Fig. 8*B*). The rounded phenotype was unlikely to be related to apoptosis, as Annexin V staining of both mock-treated and HCMV-infected LC revealed <5% annexin V-positive cells (data not shown). In addition, there was extensive overlap between loss of dendrites and detectable IE1/IE2 expression: 85% of round cells in TB40/E-exposed LC cultures were IE/IE2$^+$ by Ab staining.

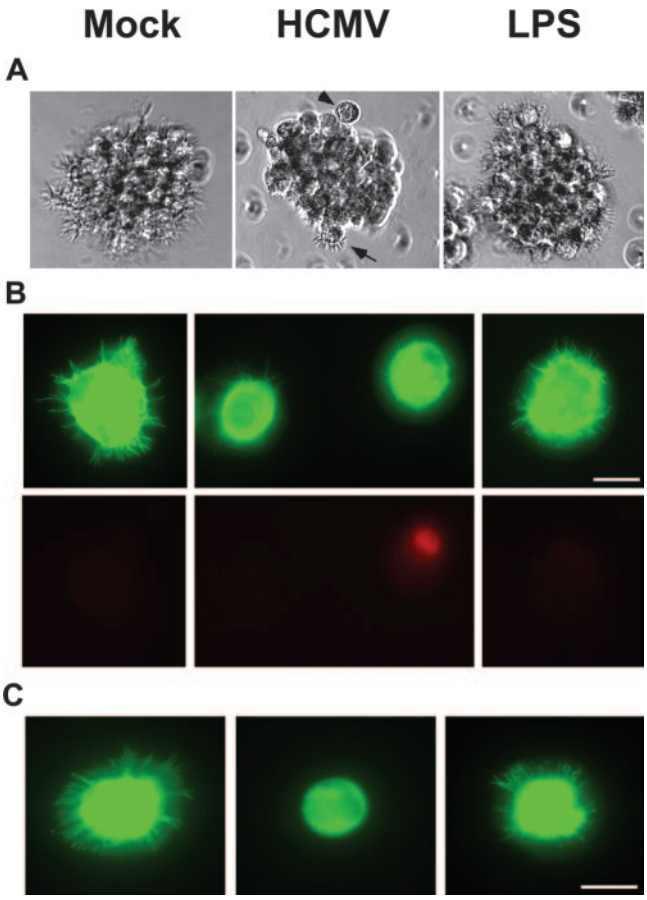

FIGURE 8. HCMV infection disrupts cytoskeletal components of dendrite architecture. Phase-contrast and IFA images of mock-infected, HCMV-infected (TB40/E MOI = 100), and LPS-treated (0.5 μg/ml) mature LC at 3 dpi. *A*, Representative phase-contrast photomicrographs of mature LC that were treated as indicated are shown. Cells were photographed in their original culture wells. Arrows and arrowheads point at dendrite-rich and dendrite-lacking cells, respectively. Original magnification, ×200. *B*, Tubulin (green) (*top*) and IE1/IE2 (red) (*bottom*) double-stained mature LC. Exposure times in the FITC channel for IE1/IE2 were kept constant across categories to allow for comparison between IE/IE2$^+$ and IE1/IE2$^-$ cells. Scale bar, 10 μm. Images are representative of three experiments with three donors. *C*, Fascin-stained mature LC. Cells were cultured and fixed as in *B*. Scale bar, 10 μm. Data are representative of two independent experiments.

Having established a correlation between HCMV infection and disruption of microtubule projections, we then investigated viral effects on the distribution of fascin, an actin bundling protein that regulates the rearrangement of cytoskeletal elements (42). As shown in Fig. 8*C*, fascin-stained mock and LPS-treated mature LC were similar in appearance, displaying multiple finger-like fascin-positive extensions beyond the cell body. In contrast, the majority of HCMV-exposed cells had a rounded phenotype, completely lacking fascin-positive projections. Taken together, these data provide strong evidence that HCMV disrupts multiple cytoskeletal elements in infected mature LC, preventing the formation or maintenance of dendrites.

Microtubules guide kinesins, motor proteins that transport MHC class II-containing vesicles to the cell surface (43). We therefore investigated whether inhibition of microtubule structure led to changes in surface expression of HLA-DR and/or other markers. Treatment of mature LC with nocodazole, a microtubule depolymerization agent (10–30 μM for 1–2 h), led to a decrease in HLA-DR surface levels (19% decrease in MFI, two experiments, data not shown), but not CD83 or MHC class I (7.5 and 17% increase in MFI, respectively). The finding of selective inhibition of HLA-DR surface expression following microtubule depolymerization suggests a mechanistic link between the HCMV effects on microtubules and on HLA-DR localization.

In vitro chemotaxis of infected mature LC

Imaging studies of live DC show "exploratory" extension of dendritic projections that precede concerted movement of the DC body (44), e.g., toward Ag-specific T cells. Therefore, we investigated whether HCMV-infected mature LC were also deficient in their ability to migrate. Mature DC express CCR7, which allows them to migrate in response to the potent chemokines CCL19 (ELC, MIP-3β) and CCL21 (SLC, 6Ckine, TCA4), which are constitutively expressed in secondary lymphoid tissue. Using a well-characterized Transwell system, we found that mock-infected mature LC migrated in response to 10 nM CCL19 or CCL21 (35 and 36% of input cells, respectively) (Fig. 9). In contrast, TB40/E-infected mature LC (MOI = 100, 3 dpi) exhibited markedly reduced chemotaxis (12 and 9% of input, respectively, $p < 0.05$ for each by *t* test) (Fig. 9). Subset analysis revealed that migration was inhibited by IE1/IE2$^+$ and IE1/IE2$^-$ mature LC exposed to HCMV. This result indicates that HCMV inhibits a key capacity of mature LC that is important for priming of T cells in vivo.

Discussion

The interaction of HCMV with DC has been an area of active investigation due to the ability of HCMV to alter the phenotype and function of these critical immune cells. We have studied in vitro-derived primary LC. These cells share many features with in vivo LC (17), which are likely to encounter virus in the body. Cultured LC allow for assessment of viral effects on constitutive MHC class II levels, free of manipulations such as transfection or IFN-γ stimulation.

A key finding of our study is that the interaction of HCMV with mature LC results in an altered distribution of HLA-DR molecules away from the cell surface, due to a block late in intracellular transport. Other studies of the interaction of HCMV and HLA class

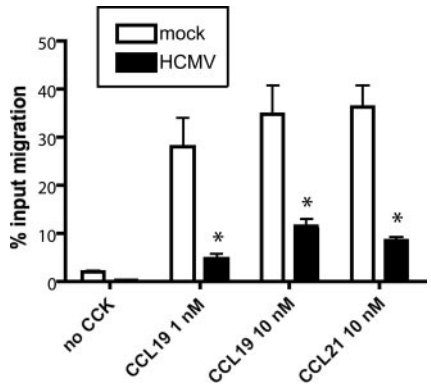

FIGURE 9. HCMV-infected mature LC exhibit reduced chemotaxis. Migration of mock- and TB40/E-infected (MOI = 100, 3 dpi) mature LC in response to chemokine. Mature LC were incubated (4 h, 37°C) in Transwell migration chambers with no chemokine, 1–10 nM CCL19, or 10 nM CCL21 in the lower chamber. Cells that migrated into the lower chamber were stained with Ab to identify mature LC and counted via flow cytometry. Each bar represents the mean percentage input migration from triplicate wells. *, Statistically significant difference from mock-treated cells ($p < 0.05$ by one-sample *t* test). One representative experiment of two is shown.

II biosynthesis in APCs also have shown reduced surface levels of HLA class II, but alternative mechanisms for this phenotype in other cell types have been identified. An HCMV-encoded IL-10 homolog was shown to block LPS-induced up-regulation of HLA class II in mature monocyte-derived DC (45). IL-10 was also implicated in reduced surface MHC class II levels on murine CMV-infected macrophages (46). In our hands, exposure to HCMV-infected mature LC medium and direct IL-10 treatment of mature LC did not recapitulate the inhibition of surface MHC class II (Fig. 2*B* and data not shown). HCMV infection of fibroblasts and endothelial cells was associated with enhanced degradation of Jak1 and consequent inhibition of IFN-γ-induced HLA class II expression (47). We also found that HCMV exposure of mature LC resulted in reduced HLA class II transcription (A. Lee, manuscript in preparation), although this did not lead to diminished total HLA-DR levels in the time frame studied (Fig. 4). The capacity of HCMV to modulate MHC class II by multiple mechanisms is reminiscent of its effects on MHC class I, which involve several HCMV proteins and different host cell targets (48).

Our knowledge of the HCMV components responsible for intracellular accumulation of MHC class II in myeloid cells remains incomplete. We found that reduction of surface HLA-DR occurred in mature LC in the absence of the US2-US11 gene products and after cell contact with live or UV-inactivated virus. HCMV tegument proteins, of which pp65 is the most abundant, are introduced into the cytoplasm of target cells directly after binding and before viral gene expression. Using a pp65-deleted, AD169-based mutant (RVAd65), we have preliminary evidence that pp65 contributes to the inhibition of HLA-DR in IE1/IE2$^-$ mature LC (data not shown). In addition, Odeberg et al. (49) found that transfection of pp65 led to reduced surface and increased perinuclear localization of MHC class II molecules in IFN-γ-treated fibroblasts. pp65 has recently been shown to inhibit components of the type I IFN response in fibroblasts and PBMC (50), but a mechanistic link to MHC class II localization remains to be identified. Work on other pathogens has revealed several nonhomologous microbial proteins, with presumably distinct host targets, that each induce intracellular accumulation of mature, peptide-loaded MHC class II molecules (51, 52). We have previously reported that pertussis toxin of *B. pertussis* contributes to retention of mature HLA-DR in primary monocytes (51). The fact that various pathogens have evolved ways to cause intracellular sequestration of peptide-loaded MHC class II suggests this may be an effective means of immune evasion.

A clue to the mechanism underlying intracellular MHC class II retention is found in our second major finding, the loss of cytoskeletal extensions in HCMV-infected mature LC. These structures normally provide support for dendrites. Microtubules also serve as the track for motor proteins called kinesins that transport MHC class II-containing vesicles to the cell surface (43). Nocodazole-mediated inhibition of microtubule polymerization led to a selective decrease in surface HLA-DR levels, arguing for a mechanistic link between cytoskeletal changes and intracellular retention of MHC class II.

Our finding that HCMV-infected mature LC lose their dendrites has important functional implications in addition to modulation of MHC class II transport. We have shown that HCMV-infected cells are markedly deficient in chemotaxis (Fig. 9). HCMV-infected monocyte-derived DC are also unable to respond to the lymphoid chemokines, attributed to a block in CCR7 expression and NF-κB signaling (53). However, in HCMV-infected mature LC, surface CCR7 levels are only modestly diminished (19), arguing for a different mechanism for their reduced migration. We propose that virally mediated inhibition of cytoskeletal elements results in both loss of dendritic spikes and reduced migratory capacity.

We and others have shown HCMV-infected DC are deficient in the stimulation of allogeneic T cell proliferation (10, 19). In monocyte-derived DC, enhanced secretion of CD95 ligand (9) (Fas ligand), and soluble CD83 (32) has been implicated, although our finding that HCMV-infected mature LC lack dendrites provides another explanation. DC lacking dendrites have reduced ability to cluster with T cells (54, 44) and depressed stimulation of allogeneic T cells (55). Recent work using two-photon laser scanning microscopy to track the physical interactions between DCs and CD8$^+$ or CD4$^+$ T cells in intact lymph nodes has also highlighted the importance of dendrites in enabling the efficient formation of immune synapses between DCs and T cells, with initial CD4$^+$ T cell-DC contacts occurring primarily at the end of dendrites (56–58).

An outstanding question is how HCMV inhibits dendrites in infected mature LC. We provide evidence that two separate cytoskeletal elements, tubulin and fascin, are unable to form projections beyond the cell body in HCMV-infected cells. Tubulin and actin are integral for cell structure and motility (59). Fascin is an actin-bundling protein that is necessary for dendrite formation in maturing DC (60). Fascin further contributes to the ability of DC to activate T cells by actively polarizing actin to form the immunological synapse (61). As we find alterations in multiple cytoskeletal elements in HCMV-infected mature LC, it is likely that HCMV interacts with a protein that regulates cytoskeletal function, rather than directly binding to the cytoskeleton itself. For example, HCMV may inhibit one or more of the GTPases required for cytoskeletal polymerization. DCs lacking the ability to form dendrites are observed in double knockout mice lacking the Rho family (GTPases) Rac1 and Rac2. DCs from these mice show severe defects in their ability to migrate toward Ag-specific T cells, and in their ability to trigger naive T cell priming in vivo (44). Intriguingly, we (L. Hertel and E.S. Mocarski, unpublished observations) have found that HCMV-infected human fibroblasts at late times postinfection have sustained reductions in transcripts encoding several Rho family GTPases (including RhoA, B, and C, Rac1, and Cdc42) and a variety of actin-modifying enzymes and GTPase-actin linking mediators (62).

One consequence of HCMV infection that could lead to dendrite loss is increased release of soluble CD83, observed in infected monocyte-derived DC (32). Notably, in a recent report from Kotzor et al. (54), treatment of monocyte-derived DC with a high concentration (10 μg/ml) of soluble CD83 resulted in dramatic changes in the distribution of multiple cytoskeletal components, including actin, tubulin, and fascin, with associated loss of dendritic veils. In future studies, it will be important to determine whether soluble CD83 mediates the striking phenotypic changes we have demonstrated.

We report that HCMV infection leads to disruption of multiple cytoskeletal elements, a novel result not previously appreciated in multiple studies of monocyte-derived DC. In summary, we have demonstrated that HCMV infection of the LC subset of DC results in intracellular retention of MHC class II, inhibition of dendritic projections, and reduced migratory function, all of which are likely to hinder critical immune functions of this cell.

Acknowledgments

We thank Tyson Holmes for helpful discussions and input regarding statistics, Brian Zabel for advice on chemotaxis assays, and Paul Roche for guidance on internalization experiments. Recombinant human CD40LT was provided by Amgen. The CD34$^+$ progenitors were provided through the National Heart Lung, and Blood Institute Programs in Excellence in

Gene Therapy Hemopoietic Cell Processing Core, and we thank Drs. Shelly Heimfeld and David Yadock (Fred Hutchinson Cancer Research Hospital, Seattle, WA) for their assistance in obtaining them. We thank Yin Dong for virus preparation. We thank Bodo Plachter (University of Mainz) for providing RVAd65; Michael Mach (University of Erlangen) for AD169*var*DE; Christian Sinzger (University of Tübingen) for TB40/E; Tom Jones (Wyeth-Ayerst Research, Pearl River, NY) for providing RV798; and William Britt (University of Alabama) for providing mAb 28-19.

Disclosures

The authors have no financial conflict of interest.

References

1. Pass, R. 2001. Cytomegalovirus. In *Fields Virology*, Vol. 2. H. Knipe, ed. Lippincott, Williams & Wilkins, Philadelphia, pp. 2675–2705.
2. Komanduri, K. V., S. M. Donahoe, W. J. Moretto, D. K. Schmidt, G. Gillespie, G. S. Ogg, M. Roederer, D. F. Nixon, and J. M. McCune. 2001. Direct measurement of $CD4^+$ and $CD8^+$ T-cell responses to CMV in HIV-1-infected subjects. *Virology* 279: 459–470.
3. Tu, W., S. Chen, M. Sharp, C. Dekker, A. M. Manganello, E. C. Tongson, H. T. Maecker, T. H. Holmes, Z. Wang, G. Kemble, et al. 2004. Persistent and selective deficiency of $CD4^+$ T cell immunity to cytomegalovirus in immunocompetent young children. *J. Immunol.* 172: 3260–3267.
4. Lucin, P., I. Pavic, B. Polic, S. Jonjic, and U. H. Koszinowski. 1992. γ Interferon-dependent clearance of cytomegalovirus infection in salivary glands. *J. Virol.* 66: 1977–1984.
5. Krmpotic, A., I. Bubic, B. Polic, P. Lucin, and S. Jonjic. 2003. Pathogenesis of murine cytomegalovirus infection. *Microbes Infect.* 5: 1263–1277.
6. Gredmark, S., and C. Söderberg-Nauclér. 2003. Human cytomegalovirus inhibits differentiation of monocytes into dendritic cells with the consequence of depressed immunological functions. *J. Virol.* 77: 10943–10956.
7. Fish, K. N., W. Britt, and J. A. Nelson. 1996. A novel mechanism for persistence of human cytomegalovirus in macrophages. *J. Virol.* 70: 1855–1862.
8. Moutaftsi, M., A. M. Mehl, L. K. Borysiewicz, and Z. Tabi. 2002. Human cytomegalovirus inhibits maturation and impairs function of monocyte-derived dendritic cells. *Blood* 99: 2913–2921.
9. Raftery, M. J., M. Schwab, S. M. Eibert, Y. Samstag, H. Walczak, and G. Schonrich. 2001. Targeting the function of mature dendritic cells by human cytomegalovirus: a multilayered viral defense strategy. *Immunity* 15: 997–1009.
10. Beck, K., U. Meyer-Konig, M. Weidmann, C. Nern, and F. T. Hufert. 2003. Human cytomegalovirus impairs dendritic cell function: a novel mechanism of human cytomegalovirus immune escape. *Eur. J. Immunol.* 33: 1528–1538.
11. Kondo, K., H. Kaneshima, and E. S. Mocarski. 1994. Human cytomegalovirus latent infection of granulocyte-macrophage progenitors. *Proc. Natl. Acad. Sci. USA* 91: 11879–11883.
12. Hahn, G., R. Jores, and E. S. Mocarski. 1998. Cytomegalovirus remains latent in a common precursor of dendritic and myeloid cells. *Proc. Natl. Acad. Sci. USA* 95: 3937–3942.
13. Söderberg-Nauclér, C., K. N. Fish, and J. A. Nelson. 1997. Reactivation of latent human cytomegalovirus by allogeneic stimulation of blood cells from healthy donors. *Cell* 91: 119–126.
14. Odeberg, J., and C. Söderberg-Nauclér. 2001. Reduced expression of HLA class II molecules and interleukin-10- and transforming growth factor β1-independent suppression of T-cell proliferation in human cytomegalovirus-infected macrophage cultures. *J. Virol.* 75: 5174–5181.
15. Tomazin, R., J. Boname, N. R. Hegde, D. M. Lewinsohn, Y. Altschuler, T. R. Jones, P. Cresswell, J. A. Nelson, S. R. Riddell, and D. C. Johnson. 1999. Cytomegalovirus US2 destroys two components of the MHC class II pathway, preventing recognition by $CD4^+$ T cells. *Nat. Med.* 5: 1039–1043.
16. Cebulla, C. M., D. M. Miller, Y. Zhang, B. M. Rahill, P. Zimmerman, J. M. Robinson, and D. D. Sedmak. 2002. Human cytomegalovirus disrupts constitutive MHC class II expression. *J. Immunol.* 169: 167–176.
17. Strobl, H., E. Riedl, C. Scheinecker, C. Bello-Fernandez, W. F. Pickl, K. Rappersberger, O. Majdic, and W. Knapp. 1996. TGF-β1 promotes in vitro development of dendritic cells from $CD34^+$ hemopoietic progenitors. *J. Immunol.* 157: 1499–1507.
18. Caux, C., B. Vanbervliet, C. Massacrier, C. Dezutter-Dambuyant, B. de Saint-Vis, C. Jacquet, K. Yoneda, S. Imamura, D. Schmitt, and J. Banchereau. 1996. $CD34^+$ hematopoietic progenitors from human cord blood differentiate along two independent dendritic cell pathways in response to $GM\text{-}CSF^+$ TNFα. *J. Exp. Med.* 184: 695–706.
19. Hertel, L., V. G. Lacaille, H. Strobl, E. D. Mellins, and E. S. Mocarski. 2003. Susceptibility of immature and mature Langerhans cell-type dendritic cells to infection and immunomodulation by human cytomegalovirus. *J. Virol.* 77: 7563–7574.
20. Strobl, H., C. Bello-Fernandez, E. Riedl, W. F. Pickl, O. Majdic, S. D. Lyman, and W. Knapp. 1997. flt3 ligand in cooperation with transforming growth factor-β1 potentiates in vitro development of Langerhans-type dendritic cells and allows single-cell dendritic cell cluster formation under serum-free conditions. *Blood* 90: 1425–1434.
21. Gatti, E., M. A. Velleca, B. C. Biedermann, W. Ma, J. Unternaehrer, M. W. Ebersold, R. Medzhitov, J. S. Pober, and I. Mellman. 2000. Large-scale culture and selective maturation of human Langerhans cells from granulocyte colony-stimulating factor-mobilized $CD34^+$ progenitors. *J. Immunol.* 164: 3600–3607.
22. Schmolke, S., H. F. Kern, P. Drescher, G. Jahn, and B. Plachter. 1995. The dominant phosphoprotein pp65 (UL83) of human cytomegalovirus is dispensable for growth in cell culture. *J. Virol.* 69: 5959–5968.
23. Jones, T. R., V. P. Muzithras, and Y. Gluzman. 1991. Replacement mutagenesis of the human cytomegalovirus genome: US10 and US11 gene products are nonessential. *J. Virol.* 65: 5860–5872.
24. Courcelle, C. T., J. Courcelle, M. N. Prichard, and E. S. Mocarski. 2001. Requirement for uracil-DNA glycosylase during the transition to late-phase cytomegalovirus DNA replication. *J. Virol.* 75: 7592–7601.
25. Hirschfeld, M., Y. Ma, J. H. Weis, S. N. Vogel, and J. J. Weis. 2000. Cutting edge: repurification of lipopolysaccharide eliminates signaling through both human and murine Toll-like receptor 2. *J. Immunol.* 165: 618–622.
26. Smith, L. M., H. R. Petty, P. Parham, and H. M. McConnell. 1982. Cell surface properties of HLA antigens on Epstein-Barr virus-transformed cell lines. *Proc. Natl. Acad. Sci. USA* 79: 608–612.
27. Morris, P., J. Shaman, M. Attaya, M. Amaya, S. Goodman, C. Bergman, J. J. Monaco, and E. Mellins. 1994. An essential role for HLA-DM in antigen presentation by class II major histocompatibility molecules. *Nature* 368: 551–554.
28. Schmid, H., M. Koop, S. Utermann, L. Lambacher, P. Mayer, and L. Schaefer. 1997. Specific catalytic activity of cathepsin S in comparison to cathepsins B and L along the rat nephron. *Biol. Chem.* 378: 61–69.
29. Busch, R., R. C. Doebele, E. von Scheven, J. Fahrni, and E. D. Mellins. 1998. Aberrant intermolecular disulfide bonding in a mutant HLA-DM molecule: implications for assembly, maturation, and function. *J. Immunol.* 160: 734–743.
30. Louie, R. K., S. Bahmanyar, K. A. Siemers, V. Votin, P. Chang, T. Stearns, W. J. Nelson, and A. I. Barth. 2004. Adenomatous polyposis coli and EB1 localize in close proximity of the mother centriole and EB1 is a functional component of centrosomes. *J. Cell Sci.* 117: 1117–1128.
31. Zabel, B. A., A. M. Silverio, and E. C. Butcher. 2005. Chemokine-like receptor 1 expression and chemerin-directed chemotaxis distinguish plasmacytoid from myeloid dendritic cells in human blood. *J. Immunol.* 174: 244–251.
32. Senechal, B., A. M. Boruchov, J. L. Reagan, D. N. Hart, and J. W. Young. 2004. Infection of mature monocyte-derived dendritic cells with human cytomegalovirus inhibits stimulation of T-cell proliferation via the release of soluble CD83. *Blood* 103: 4207–4215.
33. Cha, T. A., E. Tom, G. W. Kemble, G. M. Duke, E. S. Mocarski, and R. R. Spaete. 1996. Human cytomegalovirus clinical isolates carry at least 19 genes not found in laboratory strains. *J. Virol.* 70: 78–83.
34. Hegde, N. R., R. A. Tomazin, T. W. Wisner, C. Dunn, J. M. Boname, D. M. Lewinsohn, and D. C. Johnson. 2002. Inhibition of HLA-DR assembly, transport, and loading by human cytomegalovirus glycoprotein US3: a novel mechanism for evading major histocompatibility complex class II antigen presentation. *J. Virol.* 76: 10929–10941.
35. Jones, T. R., E. J. Wiertz, L. Sun, K. N. Fish, J. A. Nelson, and H. L. Ploegh. 1996. Human cytomegalovirus US3 impairs transport and maturation of major histocompatibility complex class I heavy chains. *Proc. Natl. Acad. Sci. USA* 93: 11327–11333.
36. Cresswell, P. 1998. Proteases, processing, and thymic selection. *Science* 280: 394–395.
37. Pious, D., L. Dixon, F. Levine, T. Cotner, and R. Johnson. 1985. HLA class II regulation and structure: analysis with HLA-DR3 and HLA-DP point mutants. *J. Exp. Med.* 162: 1193–1207.
38. Germain, R. N., and L. R. Hendrix. 1991. MHC class II structure, occupancy and surface expression determined by post-endoplasmic reticulum antigen binding. *Nature* 353: 134–139.
39. Villadangos, J. A., M. Cardoso, R. J. Steptoe, D. van Berkel, J. Pooley, F. R. Carbone, and K. Shortman. 2001. MHC class II expression is regulated in dendritic cells independently of invariant chain degradation. *Immunity* 14: 739–749.
40. Turley, S. J., K. Inaba, W. S. Garrett, M. Ebersold, J. Unternaehrer, R. M. Steinman, and I. Mellman. 2000. Transport of peptide-MHC class II complexes in developing dendritic cells. *Science* 288: 522–527.
41. Boes, M., J. Cerny, R. Massol, M. Op den Brouw, T. Kirchhausen, J. Chen, and H. L. Ploegh. 2002. T-cell engagement of dendritic cells rapidly rearranges MHC class II transport. *Nature* 418: 983–988.
42. Edwards, R. A., and J. Bryan. 1995. Fascins, a family of actin bundling proteins. *Cell Motil. Cytoskeleton* 32: 1–9.
43. Wubbolts, R., and J. Neefjes. 1999. Intracellular transport and peptide loading of MHC class II molecules: regulation by chaperones and motors. *Immunol. Rev.* 172: 189–208.
44. Benvenuti, F., S. Hugues, M. Walmsley, S. Ruf, L. Fetler, M. Popoff, V. L. Tybulewicz, and S. Amigorena. 2004. Requirement of Rac1 and Rac2 expression by mature dendritic cells for T cell priming. *Science* 305: 1150–1153.
45. Raftery, M. J., D. Wieland, S. Gronewald, A. A. Kraus, T. Giese, and G. Schonrich. 2004. Shaping phenotype, function, and survival of dendritic cells by cytomegalovirus-encoded IL-10. *J. Immunol.* 173: 3383–3391.
46. Redpath, S., A. Angulo, N. R. Gascoigne, and P. Ghazal. 1999. Murine cytomegalovirus infection down-regulates MHC class II expression on macrophages by induction of IL-10. *J. Immunol.* 162: 6701–6707.
47. Miller, D. M., B. M. Rahill, J. M. Boss, M. D. Lairmore, J. E. Durbin, J. W. Waldman, and D. D. Sedmak. 1998. Human cytomegalovirus inhibits major histocompatibility complex class II expression by disruption of the Jak/Stat pathway. *J. Exp. Med.* 187: 675–683.

48. Reddehase, M. J. 2002. Antigens and immunoevasins: opponents in cytomegalovirus immune surveillance. *Nat. Rev. Immunol.* 2: 831–844.
49. Odeberg, J., B. Plachter, L. Branden, and C. Söderberg-Nauclér. 2003. Human cytomegalovirus protein pp65 mediates accumulation of HLA-DR in lysosomes and destruction of the HLA-DR α-chain. *Blood* 101: 4870–4877.
50. Abate, D. A., S. Watanabe, and E. S. Mocarski. 2004. Major human cytomegalovirus structural protein pp65 (ppUL83) prevents interferon response factor 3 activation in the interferon response. *J. Virol.* 78: 10995–11006.
51. Shumilla, J. A., V. Lacaille, T. M. Hornell, J. Huang, S. Narasimhan, D. A. Relman, and E. D. Mellins. 2004. *Bordetella pertussis* infection of primary human monocytes alters HLA-DR expression. *Infect. Immun.* 72: 1450–1462.
52. Mitchell, E. K., P. Mastroeni, A. P. Kelly, and J. Trowsdale. 2004. Inhibition of cell surface MHC class II expression by Salmonella. *Eur. J. Immunol.* 34: 2559–2567.
53. Moutaftsi, M., P. Brennan, S. A. Spector, and Z. Tabi. 2004. Impaired lymphoid chemokine-mediated migration due to a block on the chemokine receptor switch in human cytomegalovirus-infected dendritic cells. *J. Virol.* 78: 3046–3054.
54. Kotzor, N., M. Lechmann, E. Zinser, and A. Steinkasserer. 2004. The soluble form of CD83 dramatically changes the cytoskeleton of dendritic cells. *Immunobiology* 209: 129–140.
55. Al-Alwan, M. M., G. Rowden, T. D. Lee, and K. A. West. 2001. Fascin is involved in the antigen presentation activity of mature dendritic cells. *J. Immunol.* 166: 338–345.
56. Bousso, P., and E. A. Robey. 2004. Dynamic behavior of T cells and thymocytes in lymphoid organs as revealed by two-photon microscopy. *Immunity* 21: 349–355.
57. Mempel, T. R., S. E. Henrickson, and U. H. Von Andrian. 2004. T-cell priming by dendritic cells in lymph nodes occurs in three distinct phases. *Nature* 427: 154–159.
58. Miller, M. J., O. Safrina, I. Parker, and M. D. Cahalan. 2004. Imaging the single cell dynamics of $CD4^+$ T cell activation by dendritic cells in lymph nodes. *J. Exp. Med.* 200: 847–856.
59. Pollard, T. D. 2003. The cytoskeleton, cellular motility and the reductionist agenda. *Nature* 422: 741–745.
60. Ross, R., X. L. Ross, J. Schwing, T. Langin, and A. B. Reske-Kunz. 1998. The actin-bundling protein fascin is involved in the formation of dendritic processes in maturing epidermal Langerhans cells. *J. Immunol.* 160: 3776–3782.
61. Al-Alwan, M. M., R. S. Liwski, S. M. Haeryfar, W. H. Baldridge, D. W. Hoskin, G. Rowden, and K. A. West. 2003. Cutting edge: dendritic cell actin cytoskeletal polarization during immunological synapse formation is highly antigen-dependent. *J. Immunol.* 171: 4479–4483.
62. Hertel, L., and E. S. Mocarski. 2004. Global analysis of host cell gene expression late during cytomegalovirus infection reveals extensive dysregulation of cell cycle gene expression and induction of Pseudomitosis independent of US28 function. *J. Virol.* 78: 11988–12011.